

# $\text{Cu}_x\text{SnS}_{x+1}$ ( $x = 2, 3$ ) thin films grown by sulfurization of metallic precursors deposited by dc magnetron sputtering

P. A. Fernandes, P. M. P. Salomé, and A. F. da Cunha

We report the results of the growth of Cu-Sn-S ternary chalcogenide compounds by sulfurization of dc magnetron sputtered metallic precursors. Tetragonal  $\text{Cu}_2\text{SnS}_3$  forms for a maximum sulfurization temperature of 350 °C. Cubic  $\text{Cu}_2\text{SnS}_3$  is obtained at sulfurization temperatures above 400 °C. These results are supported by XRD analysis and Raman spectroscopy measurements. The latter analysis shows peaks at 336  $\text{cm}^{-1}$ , 351  $\text{cm}^{-1}$  for tetragonal  $\text{Cu}_2\text{SnS}_3$ , and 303  $\text{cm}^{-1}$ , 355  $\text{cm}^{-1}$  for cubic  $\text{Cu}_2\text{SnS}_3$ . Optical analysis shows that this phase change lowers the band gap from 1.35 eV to 0.98 eV. At higher sulfurization temperatures increased loss of Sn is expected in the sulphide form. As a consequence, higher Cu content ternary compounds like  $\text{Cu}_3\text{SnS}_4$  grow. In these

conditions, XRD and Raman analysis only detected orthorhombic (Pmn21) phase (petrukite). This compound has Raman peaks at 318  $\text{cm}^{-1}$ , 348  $\text{cm}^{-1}$  and 295  $\text{cm}^{-1}$ . For a sulfurization temperature of 450 °C the samples present a multi-phase structure mainly composed by cubic  $\text{Cu}_2\text{SnS}_3$  and orthorhombic (Pmn21)  $\text{Cu}_3\text{SnS}_4$ . For higher temperatures, the samples are single phase and constituted by orthorhombic (Pmn21)  $\text{Cu}_3\text{SnS}_4$ . Transmittance and reflectance measurements were used to estimate a band gap of 1.60 eV. For comparison we also include the results for  $\text{Cu}_2\text{ZnSnS}_4$  obtained using similar growth conditions.

## 1 Introduction

The search for absorber layers based in  $\text{Cu}_2\text{ZnSnS}_4$  (CZTS) compounds started around a decade ago. CZTS is a p-type semiconductor and presents a high absorption coefficient, around  $10^4 \text{ cm}^{-1}$ , and a band gap around 1.5 eV [1]. Despite these properties, the  $\text{Cu}_2\text{ZnSnS}_4$  is a quaternary compound with a complex crystal structure. Associated with that complexity, the tested growth methods have shown that the crystal formation process undergoes several steps to its final form [2,3]. Unless a very controlled growth method is developed the final films may contain various spurious phases like binary and ternary sulphides.

$\text{Cu}_2\text{SnS}_3$  and  $\text{Cu}_3\text{SnS}_4$  are among the possible spurious phases.

The purpose of this work is two-fold. On one hand we study the properties of those ternary phases to understand how they may degrade the properties of the CZTS films. On the other hand we also analyse their potential to be used as cell absorbers themselves. Thus, we report the results of the growth of the ternary chalcogenide compounds,  $\text{Cu}_x\text{SnS}_{x+1}$ , where  $x=2,3$ , (CTS) by sulfurization of dc magnetron sputtered metallic precursors. The influence of the maximum sulfurization temperature on the crystallization process is investigated. We also report the results of the study of the properties of these materials focusing mostly

on those more relevant to judge their potential as cell absorbers. Compositional, morphological and structural studies of the layers are performed using SEM/EDS, XRD and Raman spectroscopy. The band gap is estimated from the transmission and reflectivity measurements. Thickness measurements are done using stylus profilometry.

## 2 Experimental details

**2.1 Sample preparation** The route followed for the deposition of the precursors, for both CTS and CZTS, is a 2-step method described elsewhere [2]. Then, the metallic precursors were deposited sequentially using dc magnetron sputtering. The deposition order used was Sn/Cu for CTS and Zn/Sn/Cu for CZTS. All depositions were done under an Ar atmosphere, an operating pressure of  $2 \times 10^{-3}$  mbar and power densities of  $0.16 \text{ Wcm}^{-2}$ ,  $0.38 \text{ Wcm}^{-2}$ ,  $0.11 \text{ Wcm}^{-2}$  for Cu, Zn and Sn, respectively. The purity of the targets was 5N for Cu and 4N for both Zn and Sn. In situ thickness' monitoring was performed with a quartz crystal monitor.

The crystal formation was performed in a tubular furnace in a  $\text{N}_2 + \text{S}_2$  vapour atmosphere at a constant working pressure of  $5.5 \times 10^{-1}$  mbar and a  $\text{N}_2$  flow rate of 40 ml/min. The sulphur pellets with purity 5N, were evaporated at 130 °C in a temperature controlled quartz tube source. The furnace temperature increases at 10 °C/min. Different maximum sulfurization temperatures were set to study its effect with the following values: 350 °C, 400 °C, 450 °C and 520 °C for CTS samples. For CZTS, the maximum temperature value was 525 °C. These temperatures were kept constant during 10 min and then the system was left to cool down naturally.

**2.2 Sample characterization** A Dektak 150 step profiler was used to measure the thickness of individual metallic precursors and the final CTS and CZTS layer thickness. In situ thickness measurement was done using a quartz crystal monitor. X-ray diffraction analysis was performed with a PHILIPS PW 3710 system equipped with a Cu-K $\alpha$  source (wavelength  $\lambda=1.54060 \text{ \AA}$ ) and the generator settings were 50mA, 40kV. A Hitachi S4100 SEM and Hitachi Su70 with a Rontec EDS with setting parameters of 25 kV and 30  $\mu\text{A}$  were used for morphological and compositional analysis. Raman scattering measurements have been performed in the backscattering configuration and the excitation laser line used was 488 nm. The Jobin-Yvon T64000 Raman spectrometer was equipped with an Olympus microscope with a 100x magnification lens. It focused the laser beam down to a spot size of 1  $\mu\text{m}$  in diameter. Optical measurements were done using a Shimadzu UV3600 spectrophotometer equipped with an integrating sphere.

The sample naming scheme uses the C and S to distinguish CTS and CZTS, respectively, followed by the maximum sulfurization temperature.

**3 Results and discussion** For the CTS samples, the composition of the precursors were set to be stoichiometric for  $\text{Cu}_2\text{SnS}_3$ . From Table 1, as expected, we see that the concentration of Sn decreases as maximum sulfurization temperature increases. The ratio [S]/Metal indicates that the samples are completely sulfurized.

**Table 1** Composition ratios based on EDS measurements.

Sample	[Cu]/[Sn]	[S]/Metal	
C350 precursors	2.1	-	
C350 sulfurized	2.3	1.1	
C400 precursors	2.0	-	
C400 sulfurized	2.1	1.0	
C450 precursors	2.0	-	
C450 sulfurized	2.6	1.1	
C520 precursors	2.1	-	
C520 sulfurized	3.2	1.1	
	[Cu]/[Zn]+[Sn]	[Zn]/[Sn]	S/Metal
S525 precursors	1.1	1.1	-
S525 sulfurized	0.9	1.1	1.1

Figure 1 shows the XRD spectra for the studied samples. The peak assignment was performed using the ICDD database [4] for tetragonal (I-42m)  $\text{Cu}_2\text{SnS}_3$ , cubic (F-43m)  $\text{Cu}_2\text{SnS}_3$ , orthorhombic (Pmn21)  $\text{Cu}_3\text{SnS}_4$  and tetragonal (I-42m)  $\text{Cu}_2\text{ZnSnS}_4$ . Figure 2 shows the detailed XRD spectra for diffraction angles,  $2\theta$ , near 47.5 °. It allows the identification of different phases. Using the parameters measured with XRD analysis, we estimated the lattice constants for each compound. For sample C350, with tetragonal unit cell structure, the lattice constants are  $a=5.41 \text{ \AA}$  and  $b=10.81 \text{ \AA}$ . Both C400 and C450, have a cubic unit cell structure with  $a=5.43 \text{ \AA}$ . The petrukite phase present in samples C450 and C520, shows the following lattice constants  $a=6.53 \text{ \AA}$ ,  $b=7.51 \text{ \AA}$  and  $c=37.76 \text{ \AA}$ . These values are in agreement with reference [4]. Note that the orthorhombic (Pmn21) phase shows a high lattice mismatch with CZTS. For this quaternary compound  $a=5.42 \text{ \AA}$  and  $b=10.87 \text{ \AA}$ .

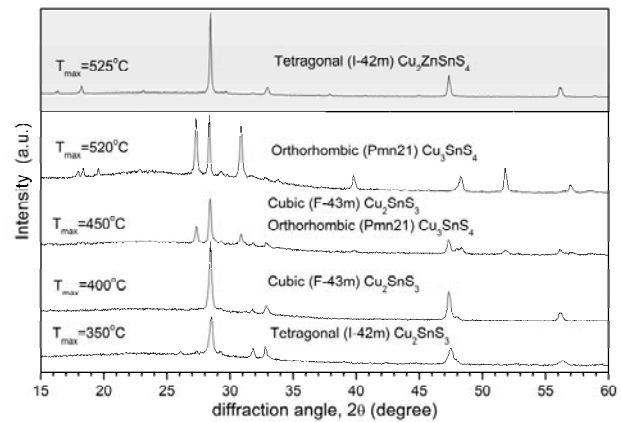


**Figure 1** XRD spectra for the CTS and CZTS samples.

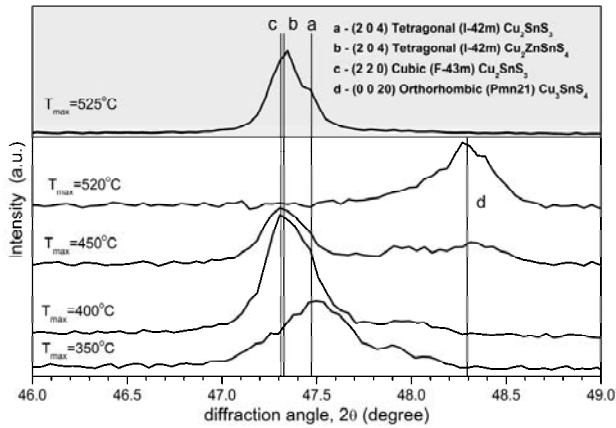


**Figure 2** Details of the XRD spectra for the CTS and CZTS samples. Peaks and Miller indices are assigned according with the reference [4].

The results of Raman spectroscopy are presented in figure 3. For the maximum sulfurization temperature of 350 °C, the Raman spectra show peaks at 336-337 cm<sup>-1</sup> and 351 cm<sup>-1</sup>. According with XRD analysis these peaks are attributed to tetragonal (I-42m) Cu<sub>2</sub>SnS<sub>3</sub>. The samples C400 and C450 show the Raman spectra for cubic (F-43m) Cu<sub>2</sub>SnS<sub>3</sub>. The main peaks for this phase are 303 cm<sup>-1</sup> and 355 cm<sup>-1</sup>. The samples C450 and C520 present peaks at 295 cm<sup>-1</sup>, 318 cm<sup>-1</sup> and 348 cm<sup>-1</sup>, which are assigned to orthorhombic (Pmn21) Cu<sub>3</sub>SnS<sub>4</sub>. No published Raman data were found for these ternary phases. The figure 3 also includes the CZTS spectrum with the main peaks at 288 cm<sup>-1</sup> and 338cm<sup>-1</sup> [2,5]. These results also show the presence of Cu<sub>2-x</sub>S with the peak at 475 cm<sup>-1</sup> [2].

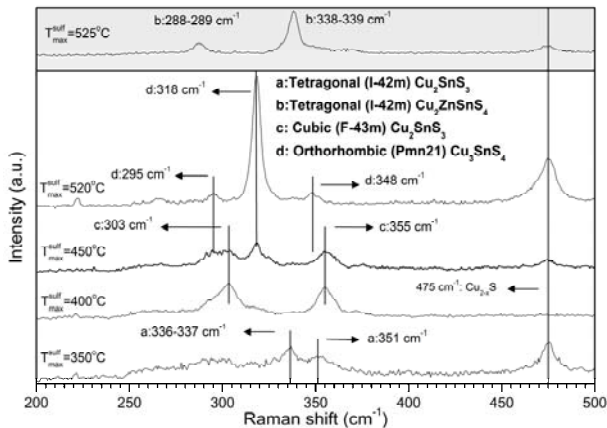


**Figure 3** Raman spectra for CTS and CZTS samples.

The samples were further studied through transmission and reflectivity measurements. The results were combined with thickness to estimate the band gap for each sample [6]. In the figure 4 we show the band gap estimations for samples C350, C400 and S525. As expected for CZTS the en-

ergy band gap is close to 1.50 eV [1]. For tetragonal (I-42m) CTS the band gap is 1.35 eV. To the best of our knowledge this value has not been reported before. It suggests possible photovoltaic applications. Cubic (F-43m) Cu<sub>2</sub>SnS<sub>3</sub> shows a band gap of 0.96 eV.

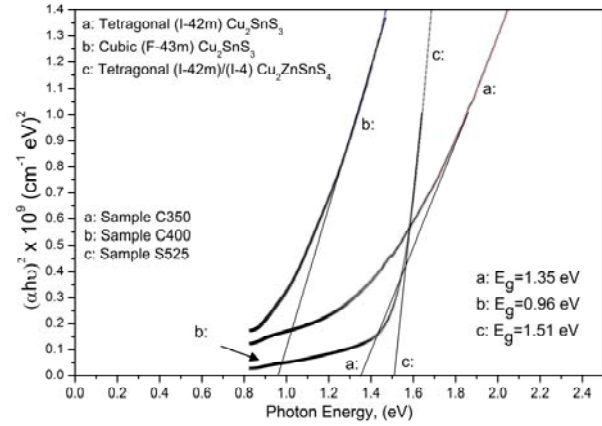


**Figure 4** Band gap estimation of the CTS samples: C350, C400 and CZTS sample: S525.

Figure 5 shows the CTS band gap estimation for the highest maximum sulfurization temperatures. The sample C520, with petrukite structure, shows a band gap of 1.60 eV. It can be seen that, for the multi-phase sample C450, this estimation is more difficult considering that we have a solid mixture of two compounds. For this sample it can be estimated a band gap at 1.55 eV assigned to orthorhombic (Pmn21) Cu<sub>3</sub>SnS<sub>4</sub> and another at 1.25 eV not assigned. This last band gap is close to tetragonal (I-42m) Cu<sub>2</sub>SnS<sub>3</sub> but XRD and Raman analysis detected no traces of this compound. To avoid the influence of the Cu<sub>2-x</sub>S, with band gaps varying from 1.3 eV to 2.3 eV [7], all these samples were etched away with KCN.

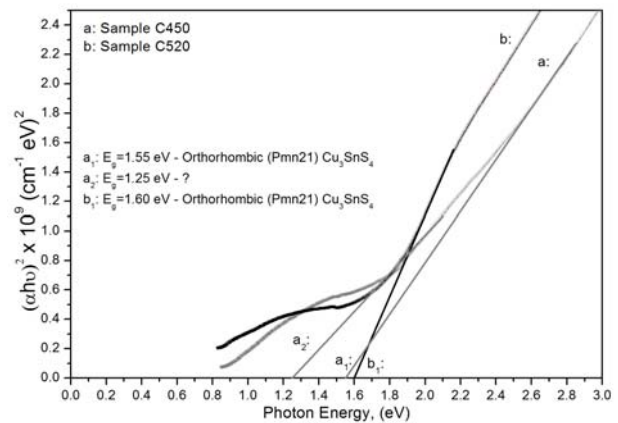


**Figure 5** Band gap estimation of the CTS samples: C450 and C520.

The morphological studies are based on the observation of SEM micrographs shown in figure 6. Micrograph a)

shows the surface of C350 sample. We can see that this sample presents a rough surface with many voids. Using this image, XRD and Raman results we can say that this layer has a poor crystalline quality. Micrograph b), corresponding to cubic (F-43m)  $\text{Cu}_2\text{SnS}_3$ , shows a more compact film, but grain size is still small. The values of FWHM of XRD and Raman peaks point to a slight improvement of the crystalline properties. Micrograph c) shows sample C450. It shows well defined crystallites intrusted in an amorphous background. Detailed EDS analysis shows stoichiometric composition for petrukite for these crystallites and for the background material is close to the cubic (F-43m)  $\text{Cu}_2\text{SnS}_3$  composition. Both compounds present poor crystalline properties. Micrograph d) shows the surface of the sample C520. It is clear that an improvement in orthorhombic (Pmn21)  $\text{Cu}_3\text{SnS}_4$  crystallinity is achieved. This statement is also supported by both XRD and Raman results. Despite this development the film presents some roughness and sparse voids.

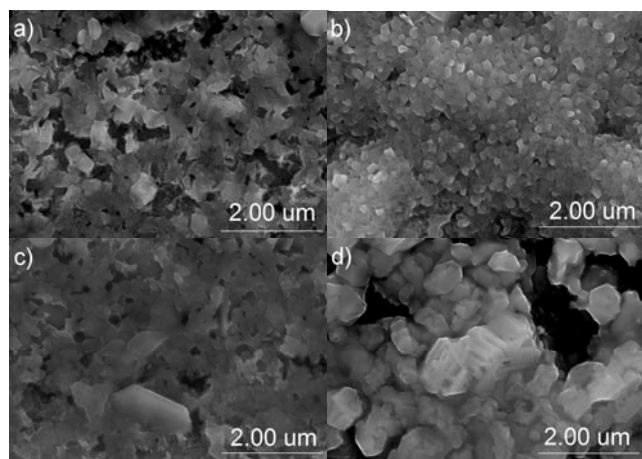


**Figure 6** Surface SEM micrographs of CTS samples: a) C343, b) C400, c) C454 and d) C518.

Figure 7 shows a surface SEM micrograph of the S525 CZTS sample. It presents a more compact and crystalline morphology. Issues concerning roughness may need some improvement.

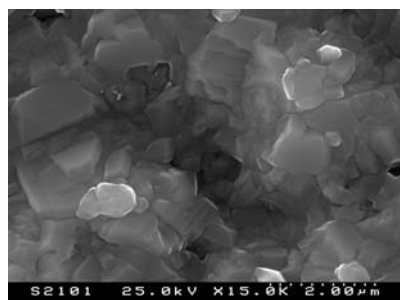


**Figure 7** Surface SEM micrograph of the S525 CZTS sample.

**4 Conclusion** In this work we studied the growth of ternary compounds and compared their properties with CZTS. For lower temperatures tetragonal (I-42m)  $\text{Cu}_2\text{SnS}_3$  forms. This compound has Raman peaks at  $336\text{--}337\text{ cm}^{-1}$  and  $351\text{ cm}^{-1}$  and a band gap of 1.35 eV. Higher temperatures result in the formation of cubic (F-43m)  $\text{Cu}_2\text{SnS}_3$  if Sn content does not drop. This phase presents Raman peaks at  $303\text{ cm}^{-1}$  and  $355\text{ cm}^{-1}$  and a band gap of 0.96 eV. Increasing further the maximum sulfurization temperature increases the evaporation of the binary sulphide SnS. This fact lowers the content of Sn helping the growth of orthorhombic Pmn21  $\text{Cu}_3\text{SnS}_4$ . No other ternary sulphide phases had been detected with any of the characterization techniques used.

No attempts were made to improve the films quality, yet, but some of these compounds present good perspectives for photovoltaic applications, especially the tetragonal (I-42m)  $\text{Cu}_2\text{SnS}_3$ . Further studies must be performed to support this statement.

The influence of these compounds in a CZTS absorber layer must be analysed separately. The tetragonal (I-42m)  $\text{Cu}_2\text{SnS}_3$  phase can not coexist with CZTS, because the CZTS temperature formation is above  $450^\circ\text{C}$ , for this growth method. Cubic (F-43m)  $\text{Cu}_2\text{SnS}_3$  can form a solid mixture with CZTS if we ensure a Sn rich precursor composition. The orthorhombic (Pmn21)  $\text{Cu}_3\text{SnS}_4$  structure may induce an increase in crystal defects due the lattice constants mismatch with CZTS. This fact would degrade the absorber layer quality. However, this phase was not detected in previous CZTS growth tests with a Cu rich precursor composition. This fact could mean preferential growth of CZTS and  $\text{Cu}_{2-x}\text{S}$  when these conditions are met.

**Acknowledgements** P.M.P. Salomé acknowledges the financial support by Fundação para a Ciência e Tecnologia, Portugal (FCT), through a PhD grant number SFRH/BD/ 29881/2006. FCT is also acknowledged for the financial support of the national electronic microscopy network whose services we have used, through the grant REDE/1509/RME/2005.

## References

- [1] J.M. Raulot, C. Domain, J.F. Guillemoles, J. Phys. Chem. Solids **66**, 2019–2023 (2005).
- [2] P.A. Fernandes, P.M.P. Salome, A.F. da Cunha, Thin Solid Films **517**, 2519–2523 (2009).
- [3] A. Weber, R. Mainz, T. Unold, S. Schorr, H. Schock, Phys. Status Solidi C **6**, 1245–1248 (2009).
- [4] International Centre for Diffraction Data - Reference Code, 04-005-0388 (CZTS), 01-089-4714 (Tetragonal I-42m  $\text{Cu}_2\text{SnS}_3$ ), 01-089-2877 (Cubic F-43m  $\text{Cu}_2\text{SnS}_3$ ), 00-36-0217 (Orthorhombic Pmn21  $\text{Cu}_3\text{SnS}_4$ ).
- [5] M. Altosaar, J. Raudoja, K. Timmo, M. Danilson, M. Grossberg, J. Krustok, E. Mellikov, Phys. Status Solidi A **205**, 167–170 (2008).
- [6] I.V. Pankove, Optical Processes in Semiconductors (Dover Inc., New York, 1975), pp. 34–95.
- [7] A. Sagade, R. Sharma, Sens. Actuators B **133**, 135–143 (2008).